Pergamon

Journal of Structural Geology, Vol. 19, No. 7, pp. 945 to 953, 1997

0191-8141/97 $17.00 + 0.00

PII: S0191-8141(97)00024-2

Fractal analysis of a Quaternary fault array in the central Apennines, Italy

GIUSEPPE CELLO

Dipartimento di Scienze della Terra, Universitá di Camerino, Via Gentile III da Varano, 62032 Camerino (MC), Italy

(*Received* 30 *September* 1996; *accepted in revised form* 6 *February* 1997)

Abstract—The Monte Vettore fault array, in the central Apennines fold and thrust belt, is part of a major Quaternary fault system displaying the main features of a regional negative flower structure associated with a roughly N–S-trending left-lateral strike–slip fault zone. Fractal analysis of the fault trace pattern of the area has shown that the box-counting curve derived for the Monte Vettore array is defined by two straight line segments, each showing a characteristic slope value. The first segment, which refers to a spatial distribution extending over about one order of magnitude, is characterized by a fractal dimension of about 1.6, whereas the second one fits a Euclidean (i.e. a non-fractal) distribution. The box-counting analysis emphasizes that faults with variable sizes exhibit different scaling relations, hence suggesting that fault linkage played a major role in the development and evolution of the Monte Vettore fault array. The split point between the two segments falls at a value of log $1/s$, corresponding to a box size of 635 m, hence suggesting that self-similarity among faults within the array breaks down below this value. Fractal analysis of the Monte Vettore array also provides statistically-based segmentation criteria for analysing a young immature fault structure capable of generating medium-size earthquakes in a continental geotectonic setting. © 1997 Elsevier Science Ltd.

INTRODUCTION

The central Apennines are part of a Neogene fold and thrust belt derived from the deformation of the southern continental margin of Neotethys. They are made up of a few main tectonic units (Fig. 1) accreted from a passive margin succession including Mesozoic and Lower Tertiary carbonate and marly formations, as well as Neogene hemipelagic and turbiditic deposits (Centamore and Deiana, 1986). These units were deformed and emplaced as a result of convergence and collision between the Corsica–Sardinia block (of European origin) and the Afro-Adriatic block (of African affinity) (Cello *et al.*, 1995b, and references therein).

The main structural features of the central Apennines fold and thrust belt consist of Late Miocene–Pleistocene thrust-related asymmetric folds (trending roughly NW–SE and N–S, depending on the structural position and age; Cello and Deiana, 1995) and faulted basement units, which are involved in the subsurface structure of the mountain chain (Lavecchia *et al.*, 1989).

Several authors (e.g. Scandone, 1979; Lavecchia, 1985; Carmignani and Kligfield, 1990) suggest that the Neogene deformation history of the Apennines is related to the opening of the Tyrrhenian basin (Kastens *et al.*, 1988) and to the inferred eastward-migrating extension driven by the flexural retreat of the lower (Afro-Adriatic) subducting plate (see also Malinverno and Ryan, 1986; Patacca and Scandone, 1989).

Cello *et al.* (1995a) show that the central sectors of the central Apennines fold and thrust belt are affected by interconnected normal, oblique and strike–slip faults belonging to a major Quaternary fault system (the Central Apennines Fault System, or CAFS), which dissects and inverts earlier thrust-related fabrics (Fig. 2). The CAFS includes several fault segments showing strong morphological evidence of Holocene activity, thus suggesting that the latter may be responsible for the moderate to strong seismic activity occurring in this sector of the Apennines (Cello *et al.*, in press). The system, as a whole, displays the main features of a negative flower structure associated with a deep-seated, roughly N–S-trending, left-lateral strike–slip fault zone. Ongoing extension and associated seismic energy release in the area occur, therefore, within this transtensional zone and do not appear to be connected to any Tyrrhenian-related extensional process.

Cello *et al.* (in press) also argue that the CAFS consists of a network of faults that are arranged in discrete fault arrays (i.e. a combination of kinematically compatible, linked, fault segments) resulting from left-lateral motion on some of the major N–S-trending structures within the system.

The aim of this contribution is to analyse one of the better-studied Quaternary fault arrays within the CAFS (i.e. the Monte Vettore fault array; Figs 2 and 3) in order to evaluate the possibility of deriving appropriate scaling relationships among the differently-sized structures making up the array, by means of fractal analysis of the fault trace pattern of the area.

THE MONTE VETTORE FAULT ARRAY

The Monte Vettore fault array dissects the hanging wall of the Monti Sibillini thrust (Fig. 2), a Late Miocene–Early Pliocene tectonic feature separating a few kilometres thick, folded carbonate and marly succession, from Mio-Plio-Pleistocene turbiditic strata

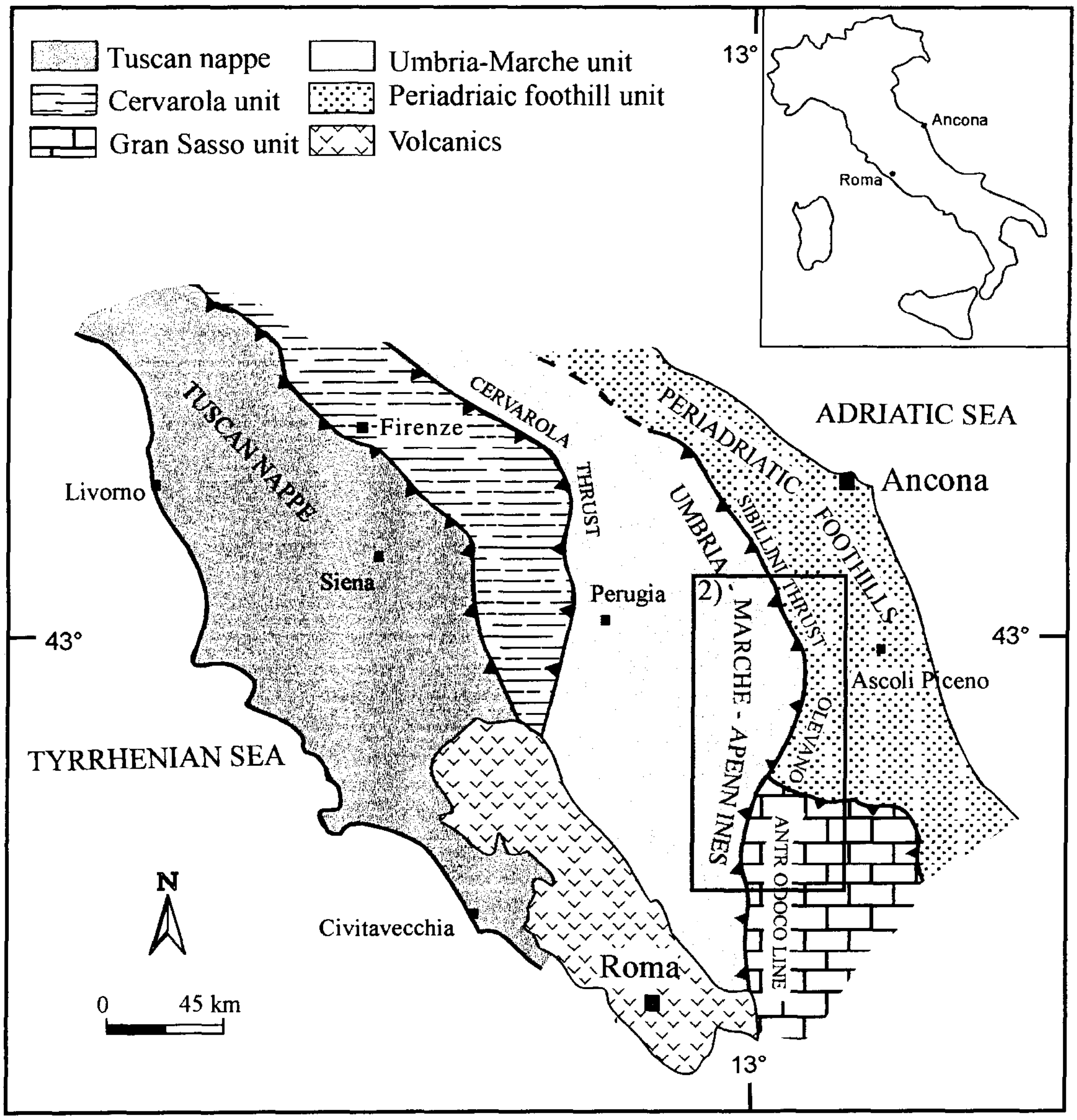

Fig. 1. Location map and tectonic sketch of the central Apennines.

of the Apenninic foredeep–foreland system of central Italy (e.g. Calamita *et al.*, 1994).

The Monte Vettore fault array developed at the northern termination of the eastern border fault of the Central Apennines Fault System. The array is made up of several fault segments that, because of their relevance for seismic hazard assessment, have been mapped in detail by means of remote sensing analysis (from Landsat images and 1:33,000 and 1:12,000 airphotos) and by accurate field work mostly based on official IGM topographic maps on a scale of 1:25,000 (Cello *et al.*, 1995a).

Photographically derived sections on a scale of 1:10,000 (covering about 30% of the territory) were also used, together with very detailed topographic profiles carried out across major fault scarps (Cello *et al.*, 1995a), to constrain better the morphotectonic characters of some of the active faults in the array (Cello *et al.*, in press).

Exposures of the Monte Vettore fault array within the high-topography zone bordering the Castelluccio basin (Fig. 2) are extremely good, thus ensuring that almost no unmapped ground was left out from the analysis, and that all fault segments larger than a few hundred metres in length were actually mapped.

The results of this work are summarized in the simplified map of the CAFS (Fig. 2) and in the digitized version (Fig. 3) of the map by Calamita *et al.* (1992), originally drawn on a scale of 1:25,000. As can be seen from these maps, the fault structure of the Monte Vettore area consists of two main NNW–SSE trending fault zones: one running along the western slope of Monte Vettore, and another more poorly developed zone bordering the Castelluccio basin to the west. The Monte Vettore fault array, as a whole, is characterized by a fault trace pattern dominated by pervasive linkage among fault segments of various lengths making up geometrically complex, differently-sized, minor fault zones within the array.

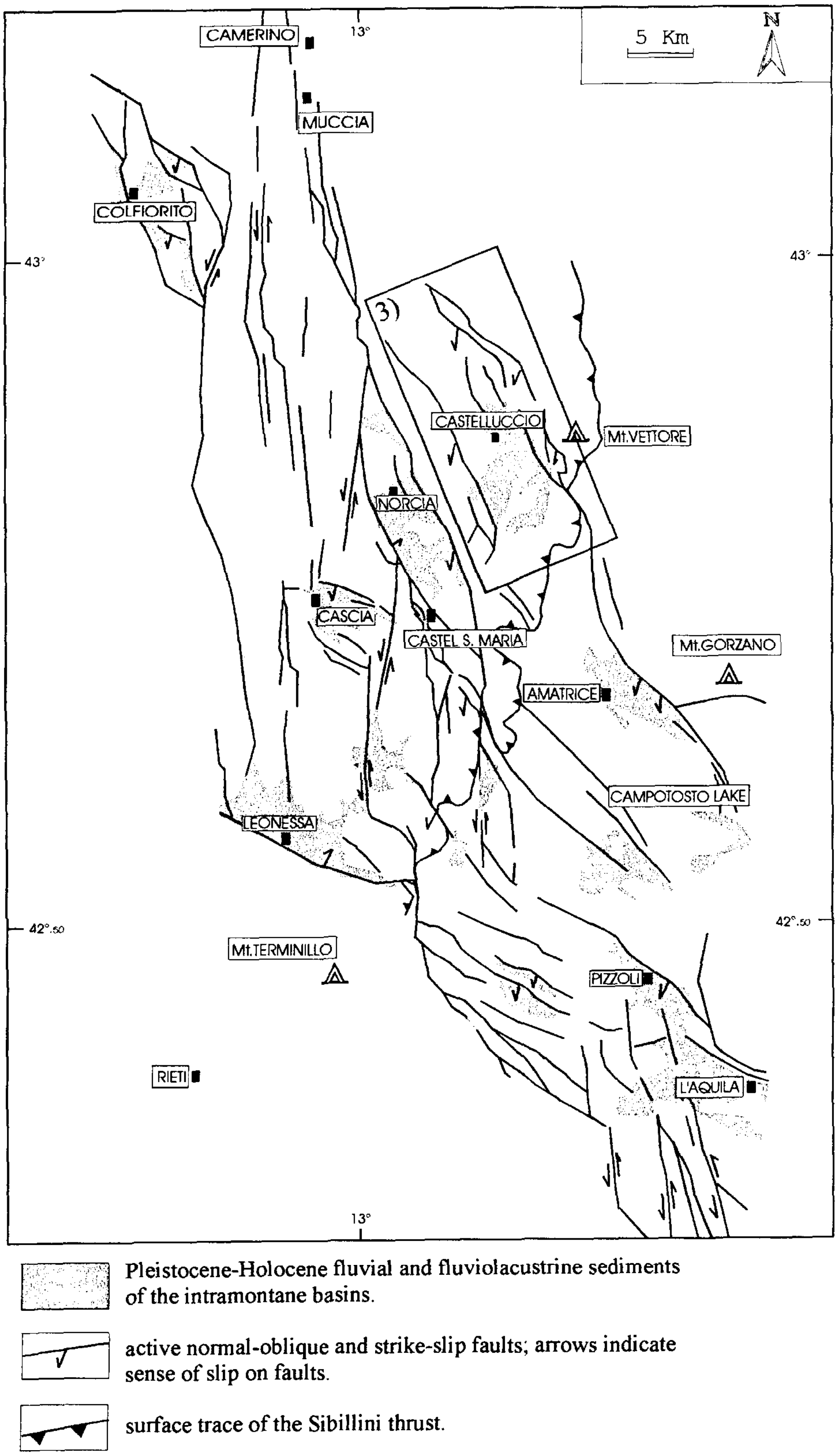

Fig. 2. The Central Apennines Fault System.

Age constraints for the Monte Vettore fault array are given by the observed cross-cutting relationships between the fault segments of the array and pre-existing compressional fabrics related to the emplacement of the Monti Sibillini thrust sheet. The most obvious situation is that occurring south of Monte Vettore, where a transtensional (left-lateral) fault offsets the main thrust surface for about 300 m (Fig. 2).

Additional evidence for Late Quaternary activity (post-700 ka) on some of the fault segments in the array,

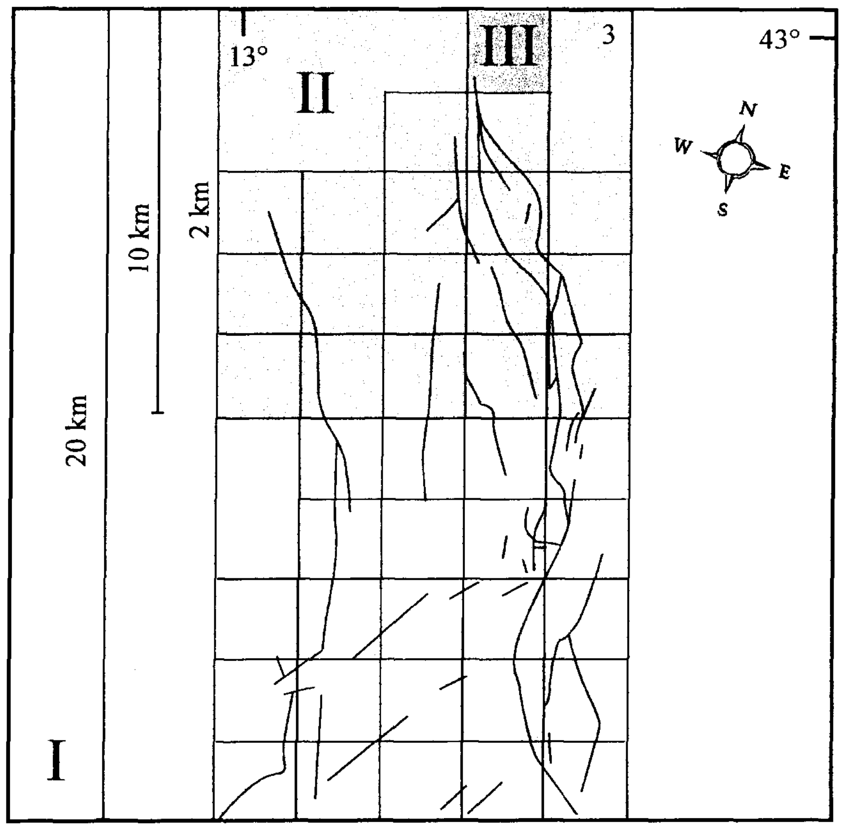

Fig. 3. The Monte Vettore fault array (digitized from the 1:25,000 scale map of Calamita *et al.*, 1992). 1, 2, and 3 show different configuration models for box-counting analysis (see text for discussion).

is given by the existence of faulted Middle Pleistocene–Holocene fluvial and fluvio-lacustrine deposits of the Castelluccio and other intramontane basins occurring within the CAFS (Blumetti, 1995; Cello *et al.*, 1995a, and references therein).

FRACTAL ANALYSIS

Areal fractal patterns of faults and fractures are conventionally analysed by box-counting techniques (Turcotte, 1992; Barton and La Pointe, 1995) which allow one to draw log/log plots of the number of boxes containing the structure (Ns) against the size of the measuring grid (s), or its reciprocal ($1/s$), and to derive box-counting curves that typically show slope values between 1 and 2 (Mandelbrot, 1983). For any pattern to be considered fractal, the box-counting curve (or part of it) needs to be a straight line defined by the following relation: $\log(Ns) = a + k\ \log(1/s)$, where the slope of the line (k) represents the fractal dimension of a given array. Map patterns with $k = 1$ have Euclidean statistical dimensions, and therefore may not be considered to be fractals.

Recent work on different fracture and fault attributes shows that they generally display a linear size–frequency relation with a fractional slope value in log/log space (Cowie *et al.*, 1996 and papers therein).

The analysis of the M. Vettore fault array was carried out by performing different box-counting measurements in order to test the relative importance of various factors on the degree of linearity of the correlation curve (i.e. to evaluate to what extent this fault array might be considered to be fractal).

To approach the problem of evaluating what starting dimension of the counting box would be most appropriate for minimizing the effects of possible unfaulted ground in our digitized map (Peitgen *et al.*, 1992), three configurations were first analysed (Fig. 3):

(1) a single box with 20-km sides;
(2) two boxes each with 10-km sides;
(3) a 39-box configuration to fit the fault array with a box side of 2 km.

The resulting box-counting curves do not show any significant difference (see curves A, B, and C, in Fig. 4); they all have fractal dimensions of approximately 1.3 and correlation coefficients (r) higher than 0.9. Accordingly, the initial dimension of the counting box was considered to be not relevant for fractal analysis of the Monte Vettore fault array.

Subsequent work was then focused on analysing in more detail configuration 2, by increasing the number of counting boxes (i.e. the number of data points in the log/log diagram). Real data sets, in contrast with computer-generated fractal structures (where the fractal dimension is given by the limit of the counting box size tending to zero; Barton, 1995) have, in fact, finite size limits (Pruess, 1995). Consequently, the number of counting boxes is

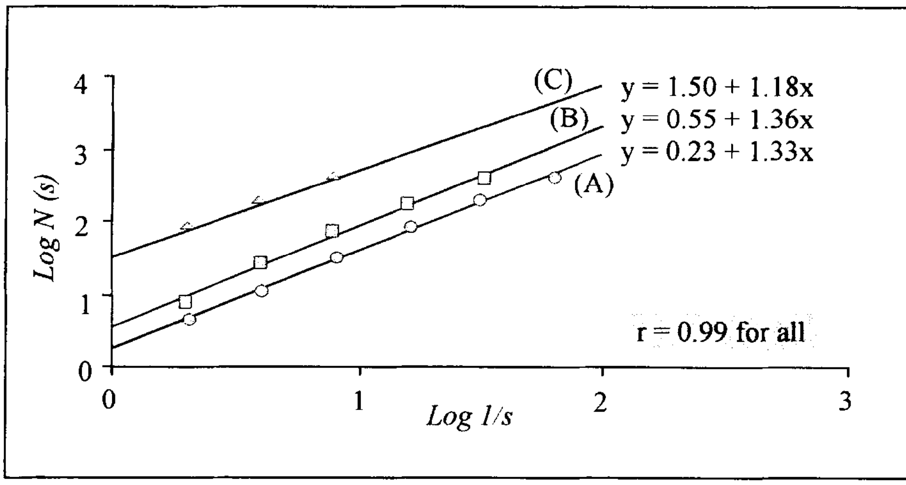

Fig. 4. Box-counting curves for configurations 1 (line A), 2 (line B), and 3 (line C).

relevant in fractal analysis of fracture and fault patterns because of the concept of validity range introduced by Walsh and Watterson (1993). The validity range concept states that there is a valid range of box dimensions which is bounded by the maximum and minimum sizes of the faults to be analysed and, as a result, regression should be considered valid only over this range.

Within the Monte Vettore fault array, maximum and minimum sizes of the faults range from approximately 18 km to a few hundreds of metres, respectively. Hence, in order to increase the number of boxes within the valid range (particularly at smaller scales: i.e. for fault lengths below 1.2 km, a value corresponding to the smallest box dimension in curve B of Fig. 4), four additional points were derived by computer-processing of the original map in Fig. 3. In practice, since it was not possible to reduce the counting box size further, the procedure adopted to obtain more points from the digitized map was that of dividing it into two boxes and doubling them to a single module. Each box was then counted separately and the values added to give a total. The procedure was repeated several times, so that each new module was progressively halved in size (halving of the box dimension producing four boxes at each step). As a result, four more data points were obtained, and the resolution of the box-counting analysis improved.

The box-counting curve obtained by using the new nine-point data set is shown in Fig. 5. The main difference between the regression line B in Fig. 4 (obtained with five points only) and that shown in Fig. 5 is given by the appearance of a definite curvature of the nine-point data set. If this curvature is real and continuous over the whole range of measurements, then the analysed fault pattern must be considered non-fractal, despite the fact that the regression line D, in Fig. 5, still has a correlation coefficient of 0.9 (see also Nicol *et al.*, 1996).

Two contrasting results therefore seem to emerge from our box-counting curves:

(1) The curves in Fig. 4 strongly suggest that the fault array is fractal over the whole range of measurements (i.e. over three orders of magnitudes) and that it is characterized by a mean fractal dimension of about 1.3.

(2) The curve D, in Fig. 5, highlights a non-linear distribution, and hence a non-fractal geometry, of the fault structure.

In my opinion, a third possibility exists, i.e. that the contradictory viewpoints outlined above result from the complexity of the object being analysed. Since we are analysing a poorly developed fault structure with a precise statistical tool, it might be possible, in fact, that the degree of complexity of the Monte Vettore fault array can be detected by variations in the fractal dimension of different components of the structure. In other words, this might mean that the curvature observed in Fig. 5 may not be real and continuous over the whole range of measurements, but that it can possibly break into discrete portions (segments) each characterized by its own slope value.

In order to test this hypothesis, the latter possibility was further investigated. Figures 6 and 7 show the results of a best-fit analysis applied to the nine-point data set. As can be seen from Fig. 6, the point distribution (as a whole) can be described by a power curve with a fractional exponent (note that this function, being non-linear in a log/log space, would suggest a non-fractal geometry of the analysed fault pattern). It must be stressed, however, that the power curve fits the points lying in those sectors of the diagram characterized by log $1/s > 1$, much better and more accurately than all the others.

Figure 7 shows the end-result of several trials aimed at discriminating among possible different segments within the same nine-point data set. Available data allow one to identify two segments showing a marked difference in slope values; the first segment is characterized by a slope (i.e. a fractal dimension) of about 1.6, whereas the second one is defined by a straight line segment with a slope of approximately 1. The latter distribution, being character-

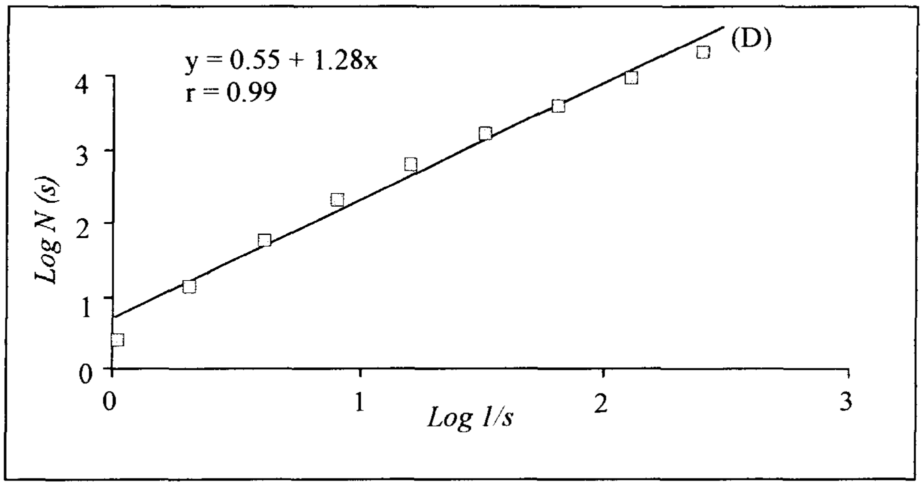

Fig. 5. Box-counting curve (line D) with nine points for configuration 2.

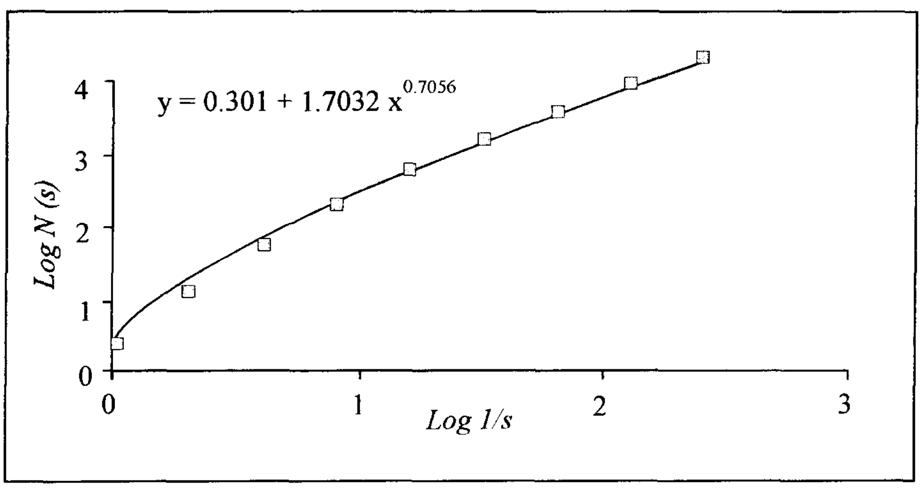

Fig. 6. Power curve fit to the nine-point data set.

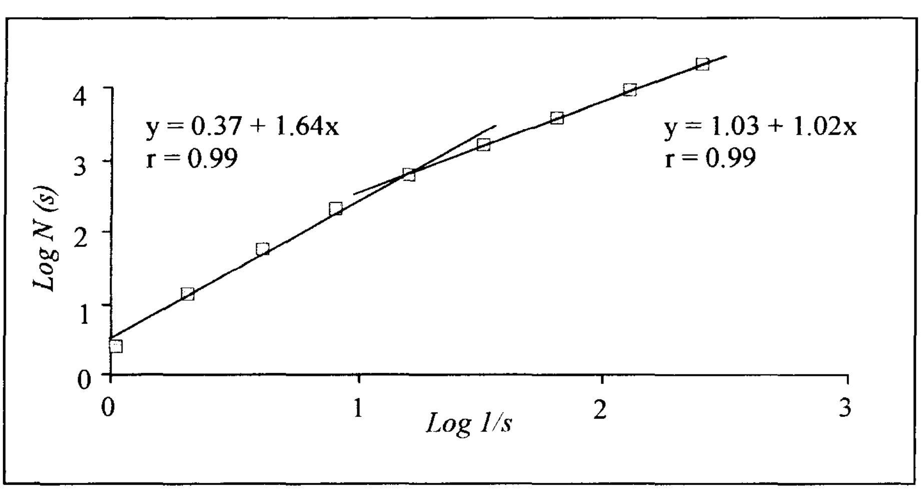

Fig. 7. Split curve fit to the nine-point data set.

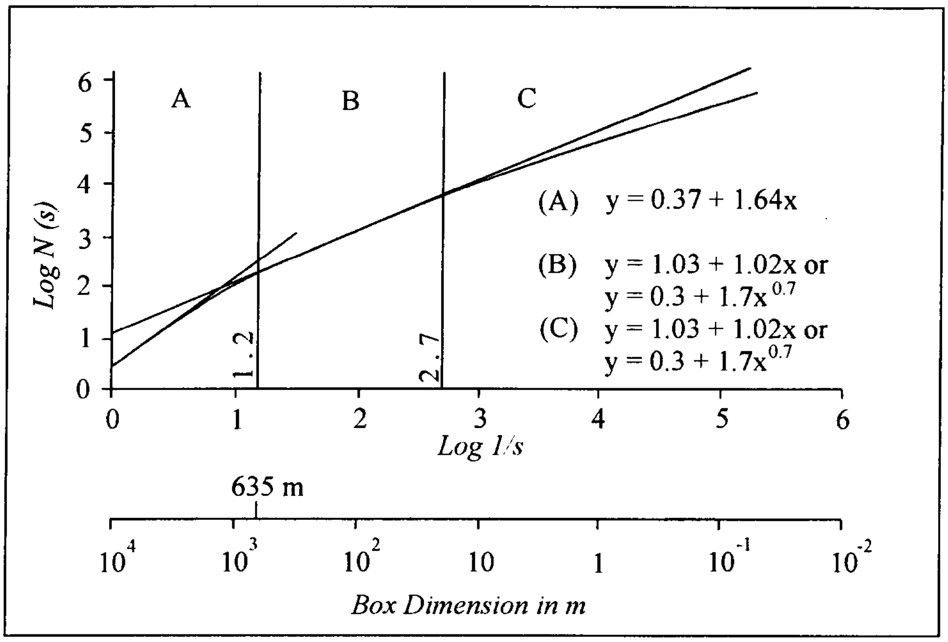

Fig. 8. Composite diagram showing three sectors displaying different scaling relations (see text for discussion).

ized by an Euclidean linear dimension, is obviously non-fractal.

The two solutions shown in Figs 6 and 7 are plotted together in Fig. 8, where extensions of both the segmented and continuous curves derived above are shown over a wider range of log $1/s$ values.

Figure 8 shows three sectors limited by different values of log $1/s$. The first one, composed of log $1/s$ values from 0 to 1.2, is bounded by a straight line segment of the box-counting curve displaying a fractal dimension of about 1.6. The middle sector (comprising values from 1.2 to 2.7) is characterized by the complete overlap between a straight line segment with a slope of about 1 and the power curve, thus suggesting that this segment is obviously not fractal, since the point distribution can be fitted either by a power curve or by a segment with a Euclidean linear dimension. For the third sector (with log $1/s$ values above 2.7) it cannot be specified whether it is bounded by the straight line with a slope of about 1 or by the power curve. In both cases, however, the segment is non-fractal.

As a result of the tests performed on the nature of the function relating the point distribution obtained from box-counting analysis of the Monte Vettore fault array, it can be emphasized, therefore, that the whole pattern may be described by two segments each showing its own slope value.

DISCUSSION AND CONCLUSIONS

Box-counting analysis of the Monte Vettore fault array, in the central Apennines, yields a log/log plot with two distinct straight line segments, hence implying that faults of different size display different scaling behaviour. Other indications resulting from the fractal analysis presented here suggest the following:

(1) The starting dimension of the counting box is not relevant in fractal analysis of faults belonging to the Monte Vettore array.

(2) A very high correlation coefficient ($r > 0.9$) for a straight-line best fit from log (Ns) vs. log ($1/s$) plots is not sufficient, in itself, to ascertain the fractal nature of fracture and fault patterns (see also Walsh and Watterson, 1993).

(3) An increase in the number of boxes used for fractal analysis of faults and fractures helps to define better the validity range of the function and the possible non-linearity of the box-counting curve (see also Barton, 1995; Pruess, 1995).

(4) The non-linearity of the box-counting curve obtained for the Monte Vettore fault array might result from the complexity of this particular structure. The Monte Vettore array, in fact, being a poorly-developed fault structure, does not fill the whole space covered by the map (because here the dissection of the older thrust structure is still incomplete) but localizes the strain within two main fault zones (Figs 2 and 3). Considering that available SOC (Self Organized Criticality) models suggest that a dissipative process such as faulting evolves through the coalescence of minor fractures (Griffith, 1920) and organizes itself spontaneously up to a point where strain localizes on dominant faults with a fractal geometry (Sornette and Davy, 1991; Cowie *et al.*, 1993; Main, 1995), it follows that a given fault structure may show variable degrees of maturity before it is fully

developed. This implies that larger faults within a given array may grow by linking in such a way as to build up a fractal geometry that can be evaluated, at each developing stage, by assessing fault complexity by means of box-counting techniques applied to fault trace patterns. Other authors argue that, as fault systems evolve, the fractal dimension changes (e.g. Wojtal, 1996). Cowie *et al.* (1995) suggest that some constant value of the fractal dimension eventually may be achieved when deformation reaches saturation, because of increasing strain. In this condition, the fractal dimension may be considered as a measure of the degree of complexity of a fully developed structure. When dealing with a fault pattern that is poorly developed in the spatio-temporal domain, the point distribution, therefore, should record the low degree of maturity of the structure by displaying a fractal dimension that is lower than the characteristic dimension of that specific fault pattern (i.e. the constant fractal dimension that would define that structure if it should ever fully develop). Alternatively, where the structure has only partially evolved as a fractal system, the point distribution should define two or more patterns (each showing a characteristic box-counting distribution). In the case of the Monte Vettore fault array, two patterns have been defined (Fig. 7): the first one is characterized by a point distribution, which is fractal in nature and displays a fractal dimension of about 1.6, whereas the second one is defined by a non-fractal distribution.

(5) The split point between the segments shown in Fig. 7 falls at a value of log $1/s$ corresponding to a box size of 635 m. This suggests that self-similarity among faults within the Monte Vettore array is effective above this value, and only over about one order of magnitude. However, the geological significance of this change in fault scaling behaviour still needs to be assessed. One possibility is that, because no significant variations with such characteristic length scale are known to occur within the crust of this sector of the Apennines, changes in fault-scaling behaviour might correlate with typology and density of fault links. Similar arguments have also been used to correlate fault displacement–length ratio variations with different linkage patterns (Cowie *et al.*, 1996).

In conclusion, the box-counting analysis presented here indicates that small faults (i.e. <635 m) are, in essence, one-dimensional features in map view, whereas larger faults (i.e. >635 m) have greater roughness (complexity), and their map patterns have a fractional dimension in excess of unity. This also suggests that the analysed structure has only partially evolved as a fractal system and that larger faults have grown by linking, in order to build up their fractal geometry.

The results of this study, therefore, seem to support the hypothesis that fault linkage plays an essential role in fault mechanics (Peacock, 1991; Cartwright *et al.*, 1995; Dawers and Anders, 1995; Wojtal, 1996). The data from the Monte Vettore array suggest that fault linkage is a major controlling factor for the growth of fault arrays with fractal geometries, and that such structures evolve from lower-rank fault populations that do not necessarily need to be characterized by power law distributions. In other words, in a given tectonic setting, before faults link sufficiently, they are essentially two-dimensional features in a three-dimensional space (therefore yielding box-counting curves with slope values of about 1), whereas once they have grown by increasing linkage, they tend to fill the deforming volume and yield fractional slope values between 1 and 2.

Acknowledgements—This research was funded by MURST (Ministero dell'Università e della Ricerca Scientifica) and CNR (Consiglio Nazionale delle Ricerche, contract n. 950035). I also wish to thank D. J. Hill for introducing me to the world of fractals, and J. A. Cartwright and S. F. Wojtal for their constructive reviews.

REFERENCES

Barton, C. C. (1995) Fractal analysis of scaling and spatial clustering of fractures. In *Fractals in the Earth Sciences*, eds C. C. Barton and P. R. La Point. Plenum Press, New York.

Barton, C. C. and La Pointe, P. R. (ed.) (1995) *Fractals in the Earth Sciences*. Plenum Press, New York.

Blumetti, A. M. (1995) Neotectonic investigation and evidence of paleoseismicity in the epicentral area of the January–February 1703, central Italy, earthquake. In *Perspectives in Paleoseismology*, eds L. Serva and D. B. Slemmons, Vol. 6, pp. 83–100. Association of Engineering Geology, Special Publication.

Calamita, R., Cello, G., Deiana, G. and Paltrinieri, W. (1994) Structural styles, chronology-rates of deformation, and time–space relationships in the Umbria–Marche thrust system (central Apennines Italy). *Tectonics* **13**, 873–881.

Calamita, F., Pizzi, A. and Roscioni, M. (1992) I fasci di faglie recenti ed attivi di M. Vettore–M. Bove. *Studi Geologici Camerti* **1**, 81–102.

Carmignani, L. and Kligfield, R. (1990) Crustal extension in the Northern Apennines: the transition from compression to extension in the Alpi Apuane Core Complex. *Tectonics* **9**, 1275–1303.

Cartwright, J., Mansfield, C. and Trudgill, B. (1995) The growth of faults by segment linkage: evidence from the Canyonlands graben of S.E. Utah. *Journal of Structural Geology* **17**, 1319–1326.

Cello, G. and Deiana, G. (1995) Role and effects of pore fluid pressure in thrusting: the case history of the Umbria–Marche Apennines (central Italy). *Tectonics* **14**, 848–854.

Cello, G., Mazzoli, S., Tondi, E. and Turco, E. (1995) Tettonica attiva in Appennino centrale e implicazioni per l'analisi della pericolosità sismica del settore assiale della catena umbro-marchigiana-abruzzese. *Studi Geologici Camerti* **13**, 115–138.

Cello, G., Mazzoli, S., Tondi, E. and Turco, E. (in press) Active tectonics in the central Apennines and possible implications for seismic hazard analysis in peninsular Italy. *Tectonophysics*.

Cello, G., Turco, E. and Zuppetta, A. (1995b) Cinematica del settore centrale del Mediterraneo ed implicazioni sulla strutturazione dell'Arco Calabro. In *Cinquanta anni di Attività Didattica e Scientifica del Prof. Felice Ippolito*, eds G. Bonardi, B. de Vivo, P. Gasparini and A. Vallario, pp. 293–301. Liguori, Napoli.

Centamore, E. and Deiana, G. (1986) Geologia delle Marche. *Studi Geologici Camerti*, Vol. spec. 1986/1, 9–145.

Cowie, P. A., Knipe, R. J., Main, I. G. and Wojtal, S. F. (1996) Scaling laws for fault and fracture populations: Analyses and applications. *Journal of Structural Geology* **18**, 135–383.

Cowie, P. A., Sornette, D. and Vanneste, C. (1995) Multifractal scaling properties of a growing fault population. *Geophysics Journal International* **122**, 457–469.

Cowie, P. A., Vanneste, C. and Sornette, D. (1993) Statistical physics model for the spatiotemporal evolution of faults. *Journal of Geophysical Research* **98**, 21809–21821.

Dawers, N. H. and Anders, M. H. (1995) Displacement–length scaling and fault linkage. *Journal of Structural Geology* **17**, 607–614.

Griffith, A. A. (1920) The phenomenon of rupture and flow in solids. *Philosophical Transactions of the Royal Society of London, A* **221**, 163–198.

Kastens, K., Mascle, J., Auroux, C., Bonatti, E., Broglia, C., Channell, J. E. T., Curzi, P., Kay-Christian, E., Glacon, G., Hasegawa, S., Hieke, W., Mascle, J., McCoy, F., McKenzie, J., Mendelson, J., Muller, C., Rehault, J.-P., Robertson, A., Sartori, R., Sprovieri, R. and Torii, M. (1988) ODP Leg 107 in the Tyrrhenian Sea: Insights into passive margin and back-arc basin evolution. *Geological Society of America Bulletin* **100**, 1140–1156.

Lavecchia, G. (1985) Neogene-Quaternary evolution of the Tyrrhenian-Apennine system. *Memorie della Società Geologica italiana* **30**, 213–214.

Lavecchia, G., Minelli, G. and Pialli, G. (1989) Contractional and extensional tectonics along the transect Lake Trasimeno-Pesaro (central Italy). In *The Lithosphere in Italy. Advances in Earth Sciences Research*, eds A. Boriani, M. Bonafede, G. B. Piccardo and G. B. Vai, Vol. 80, pp. 177–194. Accademia Nazionale dei Lincei, Rome.

Main, I. G. (1995) Seismogenesis and seismic hazard. *Proceedings VIII* Summer School Earth and Planetary Sciences on 'Plate Tectonics: The First Twenty-Five Years' Siena, Italy, pp. 395–419.

Malinverno, A. and Ryan, W. B. F. (1986) Extension in the Tyrrhenian Sea and shortening in the Apennines as result of arc migration driven by sinking of the lithosphere. *Tectonics* **5**, 227–245.

Mandelbrot, B. B. (1983) *The Fractal Geometry of Nature*. W. H. Freeman, New York.

Nicol, A., Walsh, J. J., Watterson, J. and Gillespie, P. A. (1996) Fault size distributions—are they really power law? *Journal of Structural Geology* **18**, 191–197.

Patacca, E. and Scandone, P. (1989) Post-Tortonian mountain building in the Apennines: the role of the passive sinking of a relic lithospheric slab. In *The Lithosphere in Italy. Advances in Earth Sciences Research*, eds A. Boriani, M. Bonafede, G. B. Piccardo and G. B. Vai, Vol. 80, pp. 157–176. Accademia Nazionale dei Lincei, Rome.

Peacock, D. C. P. (1991) Displacements and segment linkage in strike-slip fault zones. *Journal of Structural Geology* **13**, 1025–1035.

Peitgen, H. O., Jurgens, H. and Saupe, D. (1992). *Chaos and Fractals: New Frontiers of Science*. Springer, New York.

Pruess, S. A. (1995) Some remarks on the numerical estimation of fractal dimension. In *Fractals in the Earth Sciences*, eds C. C. Barton and P. R. La Point. Plenum Press, New York.

Scandone, P. (1979) Origin of the Tyrrhenian Sea and Calabrian Arc. *Bollettino della Società Geologica italiana* **98**, 27–34.

Sornette, D. and Davy, Ph. (1991) Fault growth model and universal fault length distribution. *Geophysics Research Letters* **18**, 1079–1081.

Turcotte, D. L. (1992) *Fractals and Chaos in Geology and Geophysics*. Cambridge University Press, Cambridge.

Walsh, J. J. and Watterson, J. (1993) Fractal analysis of fracture patterns using standard box-counting techniques: valid and invalid methodologies. *Journal of Structural Geology* **12**, 1509–1512.

Wojtal, S. F. (1994) Fault scaling laws and temporal evolution of fault systems. *Journal of Structural Geology* **16**, 603–612.

Wojtal, S. F. (1996) Changes in fault displacement populations correlated to linkage between faults. *Journal of Structural Geology* **18**, 265–279.